



SEISMIC RESPONSE EVALUATION OF ZONAL HANGING CURTAIN WALL SYSTEM USING HYBRID SIMULATION

Y.L. Wang⁽¹⁾, K.M. Mosalam⁽²⁾, S. Günay⁽³⁾ and W.S. Lu⁽⁴⁾

⁽¹⁾ Ph.D. Candidate, Tongji Univ., China & Visiting Student, PEER, Univ. of California, Berkeley, USA, wangyangling99@gmail.com

⁽²⁾ Taisei Professor of Civil Eng., Dept. of Civil & Environmental Eng., Univ. of California, Berkeley, USA, mosalam@berkeley.edu

⁽³⁾ Project Scientist, Dept. of Civil and Environmental Eng., Univ. of California, Berkeley, USA, selimgunay@berkeley.edu

⁽⁴⁾ Professor, College of Civil Eng., Tongji Univ., Shanghai, China, wally@tongji.edu.cn

Abstract

The outer curtain wall system of Shanghai Tower adopts flexible zonal hanging glass curtain wall (CW) system, which is vertically hung from the suspension beam of the mechanical floor by sag rods. Due to the irregular plan configuration of this CW supporting structure (CWSS), the overhang length of the suspension beam changes in different hanging points, which affects the seismic behavior of the CWSS. Therefore, it is necessary to investigate the influence of the suspension beam stiffness on the behavior of the CWSS under vertical seismic inputs. For this purpose, a simplified 2D model of the CWSS, which focuses on the suspension beam and sag rods, was developed first. Subsequently, a parametric study was carried out to investigate the effect of the suspension beam stiffness, utilizing this CWSS model with acceleration inputs from the corresponding hanging floor obtained from nonlinear analysis of the main structure under design earthquake motions. The parametric study results identified the critical configuration of this CWSS, where the stiffness ratio between the suspension beam and sag rod is 0.1. Nonlinear analyses of the simplified CWSS (SCWSS) for the stiffness ratio of 0.1, with four different inputs, were performed to determinate the critical sag rod position. The results showed that the sag rod in the hanging position exhibits nonlinear behavior prior to other sag rods. Different from the shaking table tests focusing on the seismic performance of CW panels, the hybrid simulation (HS) method was employed herein to evaluate the vertical seismic performance of the most critical configuration of the SCWSS. The HS tests were conducted using the HS system in the Structural Laboratory in the University of California, Berkeley. In the tests, the sag rod in hanging position, determined to be the most critical element from nonlinear analyses, was simulated as an experimental substructure, while the other rods were analytically modeled in OpenSees. Considering the setup capacity and the test purpose, the test specimen was designed to meet the requirements of force-displacement similitude with a length scale factor of 13.0. Other similitude relations were dictated by the material properties of the test specimen, determined before the HS tests. The HS tests with the input of three intensity scenarios, namely frequent, precautionary and rare earthquakes of intensity 7 (based on the Chinese design code), were carried out. The results from the HS tests and pure analysis were compared and it was observed that the HS results matched quite well with the analytical results when the specimen was elastic. With respect to the input of rare intensity, differences appeared between the HS and the analytical simulations after specimen yielding due to uncaptured sources of inelasticity in the analytical simulations. The specimen buckled under the input of rare intensity with maximum full-scale deformation of 64.5 mm before breaking, which is expected to subject the CW panel to compression in the vertical direction and may result in damage of the panel.

Keywords: hybrid simulation, parameter study, seismic response, zonal hanging CW system.

1. Introduction

Shanghai Tower, located in the Lujiazui financial center of Shanghai, is the tallest high-rise building in China with the height of 632 m, as shown in Fig. 1. The structure is divided into nine zones with number of stories varying from twelve to fifteen in each zone. It adopts a unique exterior envelop design utilizing double skin curtain wall (CW) system: the inner one uses normal frame unit curtain wall system, while the exterior one adopts the flexible zonal hanging system. In each zone, an atrium is created by the interstitial space between the inner and outer curtain wall systems, which operates as a gathering space and the center for activity within the zone community [1].

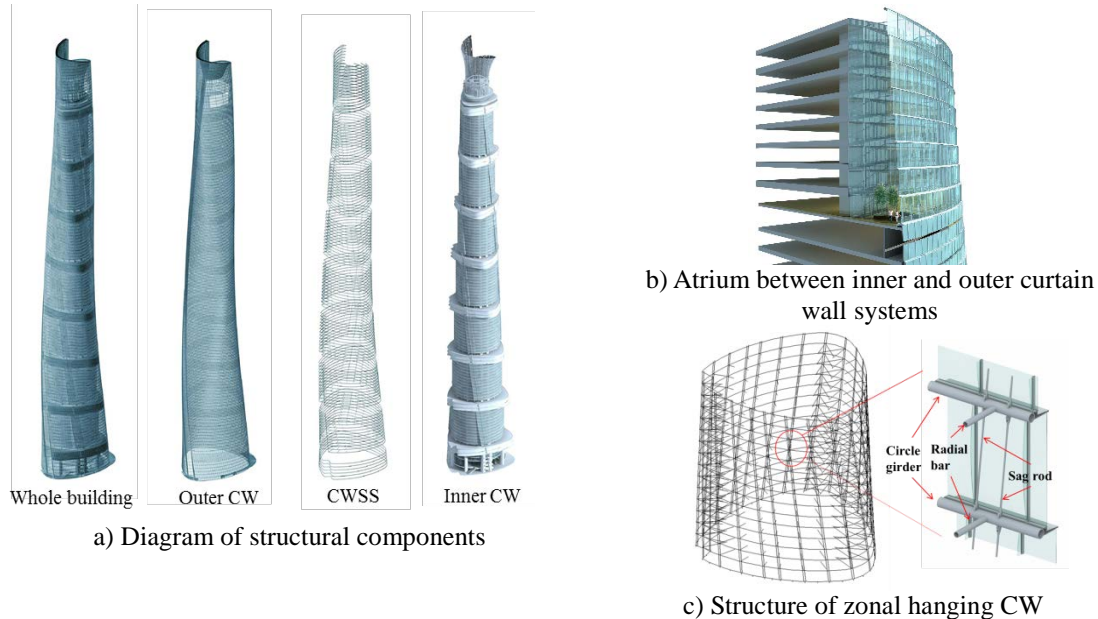


Fig. 1 – Shanghai Tower and zonal hanging CW system

The supporting system of the exterior curtain wall comprises a vertical gravity system and a horizontal system, Fig. 1. The CW is hung from the strengthening story vertically by sag rods and connected to the inner tower horizontally by radial bars. Both radial bars and sag rods are connected to the horizontal circular girder.

Several CW systems have shown their vulnerability to damage during earthquakes in the last two decades (Northridge, CA 1994 [2], San Simeon, CA 2003 [3], and Christchurch, NZ 2011 [4]). Such damage includes CW unit failures (e.g. sealant damage, panel breakage and panel fallout) and supporting system failures (e.g. anchor failure and supporting structure buckling and failure), which present a severe threat to life safety, property security and maintenance of functionality. Therefore, an elevated level of attention has been given to CW seismic performance in recent years. Most of the pioneering studies focused on the in-plane deformation performance and out-of-plane dynamic motions of CW panels using static and dynamic racking tests with different loading history [5-8]. Based on these studies, the American Architectural Manufacturer's Association (AAMA) [9-10], adopted by the International Building Code (ICC) [11] and ASCE7 [12], stipulates the test procedures for both static and dynamic loading to evaluate the in-plane drift capacity of CW panel through mock-up specimen and test setup. More recently, in order to provide more realistic performance evaluation of CW panels, shaking table tests [13-15] were conducted utilizing floor accelerations as inputs obtained from pretest analysis of the main structure subjected to ground motion.

However, most of the conducted experimental studies have been focused on the seismic performance of the CW panels and on developing general prediction models for glass cracking during seismic induced drift. Few of these studies have been conducted to investigate the seismic performance of the supporting structure of the CW, due to its large spatial configuration and the limitation of supporting devices in conventional structural testing laboratory facilities. One of the methods to overcome these limitations is hybrid simulation (HS), where

the critical components of a structure are simulated as experimental substructures with the rest simulated as analytical substructures in a computer model. Since its first introduction by Takanashi et al. [16], HS method has been extensively enhanced and widely used in investigating various complex structures, including, but not limited to, buildings with energy dissipation devices [17-19], retrofit of wood-frame buildings [20], bridges [21] and high voltage disconnect switches [22]. The HS method provides an opportunity to evaluate the system response of the whole zonal hanging CW supporting system (CWSS) as compared to limited individual component evaluations provided by quasi-static or shaking table tests.

Therefore, the HS method has been used for investigating the vertical seismic response of the zonal hanging supporting system utilized in Shanghai Tower, for which the component response of CW panels had been previously evaluated through shaking table tests [23-24]. In order to determine the critical parameters and the configuration to be tested, a pretest parametric study was initially conducted with a simplified model, as discussed in the following sections.

2. Pretest simplified model

Based on the analysis of the main structure, the peak vertical acceleration amplitude of zone 8 is the highest with values more than four times of the peak ground acceleration [25]. Therefore, the CWSS of zone 8 has been chosen as the study object in this paper. As shown in Fig. 2, due to the irregular plan configuration, the CWSS is hung to the suspension beams extended from the strengthening floor of each zone with varied overhang length, which results in the variation of the hanging stiffness and subsequently affecting the dynamic properties of the system.

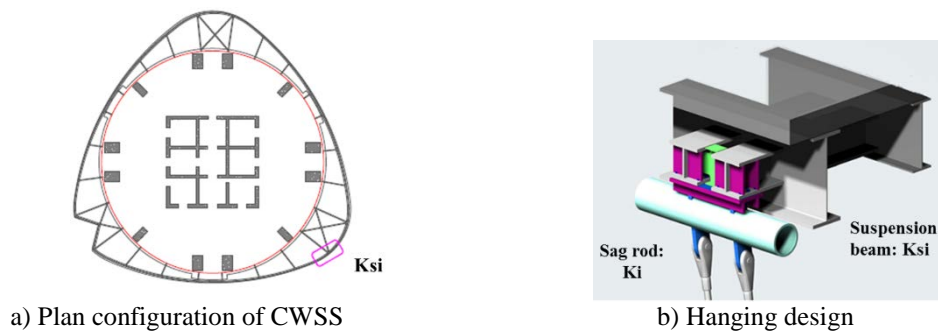


Fig. 2 – Plan configuration of CWSS and hanging design diagram

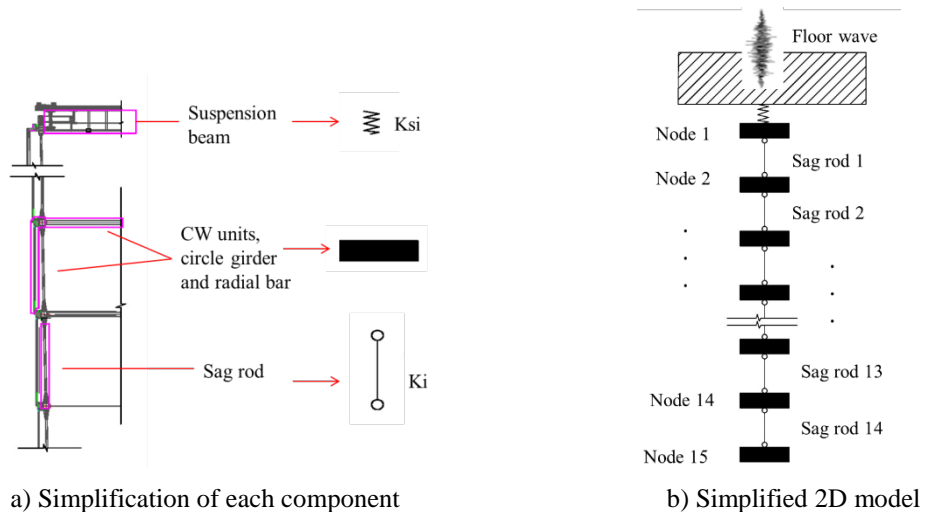


Fig. 3 – Simplification of the 3D CWSS to 2D model

In order to further explore the stiffness effect of suspension beams and the critical sag rod position, a simplified 2D model developed in OpenSees [26] was utilized in the pretest parametric study, which was essential to investigate the most severe situation to be studied in the HS test. The simplification process is illustrated in Fig. 3 and summarized as follows: (a) the suspension beam was simulated as a spring in the model with stiffness K_{si} , (b) the sag rod was modeled with a truss element with stiffness K_i , (c) since the CW unit, between adjacent circular girders, is hung on the upper level circular girder, these girders with CW units were represented as lumped mass, and (d) because the lower end of this CW system is connected to the floor by cantilever bearings, located at the lowest circle girt, which can slide up and down to accommodate the vertical movement, no vertical restraint of the end bearings was provided in the model.

3. Pretest parametric study

As indicated previously, the simplified CWSS (SCWSS) of zone 8 has been selected for investigation based on analysis of the main structure. In the parametric study of the SCWSS, which focused on the effect of the suspension beam stiffness and critical position of the sag rod, 15 different stiffness ratio values β ($\beta = K_{si} / K_i$), and 14 vertical positions, as discussed later, were considered. Four different floor accelerations (FW-US, FW-MEX, FW-SHW3, FW-S790 summarized in Table 1) were used as inputs. These accelerations are the vertical acceleration responses extracted from the corresponding hanging floor of the main structure under the corresponding four ground motions. It is noted that the acceleration response spectra of these ground motions are compatible with the spectrum of the design earthquake with peak acceleration of 0.1 g and with 10% probability of exceedance in 50 years [27].

Table 1 – Basic information of design ground motions and corresponding floor motions

Earthquake ground motion information			Corresponding floor motion	
Record	Component	Notes	Record	
Mexico city earthquake	MEX006	N00E	1985.09.19 Guerrero array, Vile, Mexico	FW-MEX
	MEX007	N90E		
	MEX008	UP		
Borrego mountain earthquake	US1215	East	1968.04.08 Hollywood storage, Los Angeles, CA	FW-US
	US1214	North		
	US1213	UP		
Synthetic record	S79010	Horizontal	Synthetic record based on site and structure responses	FW-S790
	S79011	Horizontal		
	S79012	Vertical		
DGJ08-9-2013	SHW3	-	Synthetic record based on local code [27]	FW-SHW3

Fig. 4 presents the pseudo-acceleration response spectrum of the floor motions. It is noted that the peak response is around a period of 0.58 s, which is mainly dictated by the first vertical vibration mode of the main structure, determined to be 0.65 s [25].

3.1 Effect of suspension beam stiffness

The considered stiffness ratios ranging from 1/640 to 204.8 represents different suspension beam configurations, where 1/640 presents the configuration with the most flexible suspension beam, and the largest ratio 204.8 corresponds to the situation with the largest stiffness. The fundamental periods of the SCWSS corresponding to different stiffness ratios are plotted in Fig. 5, where the natural period of the model converges to 0.35 s when the stiffness ratio is larger than 25.6.

For each stiffness ratio, nonlinear dynamic analyses of the SCWSS under the four different inputs were conducted utilizing OpenSees [26]. The acceleration amplification indices (AAI, ratio of the peak SCWSS acceleration to the peak floor acceleration) of the system and peak deformations of the sag rod for different stiffness ratios are plotted in Fig. 6. It is noted that the most severe situation occurs with the stiffness ratio of 0.1, where the corresponding AAI and peak sag rod deformation are 9.5 and 85.45 mm, respectively, and the fundamental period of the SCWSS is 0.56 s, which corresponds to the dominant frequency of the input motions, namely the SCWSS is in resonance with the floor motion at this frequency.

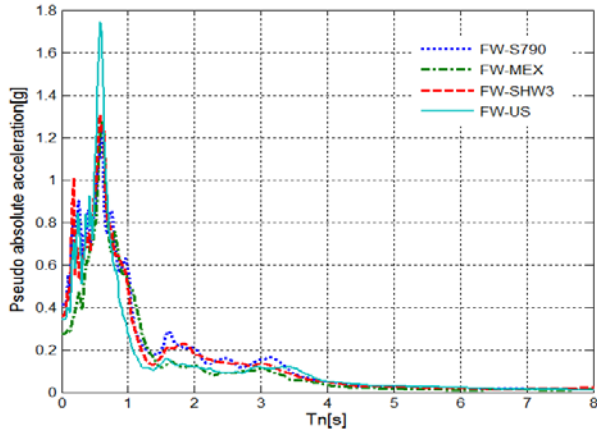


Fig. 4 –Pseudo-acceleration response spectrum of floor motions for CW system of Zone 8

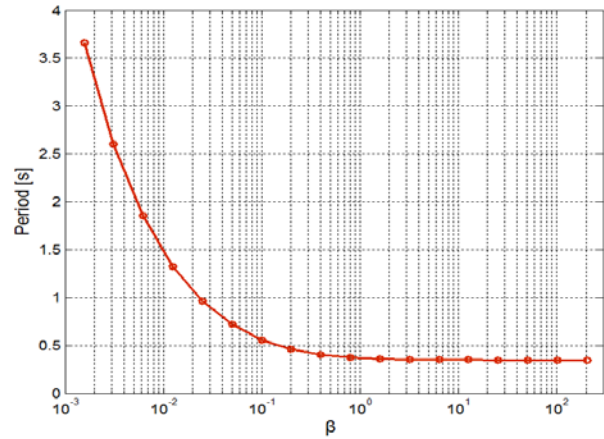
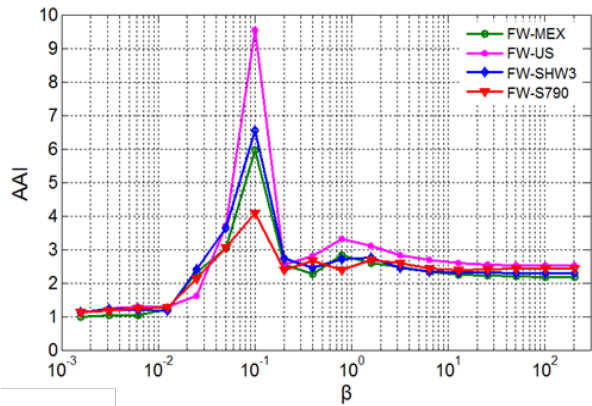
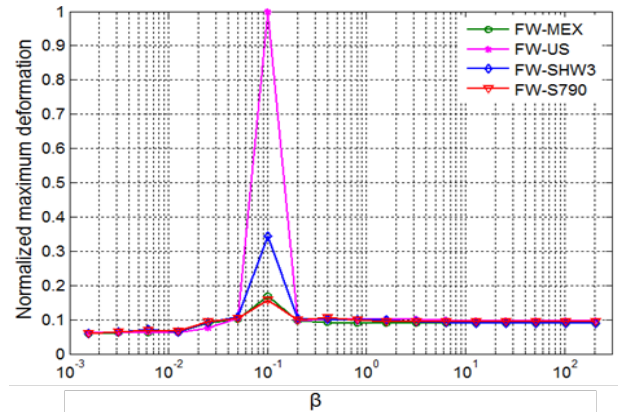


Fig. 5 –Fundamental period of the SCWSS under different stiffness ratio



a) AAI



b) Normalized maximum element deformation

Fig. 6 –Variation of AAI and normalized peak element deformation with the stiffness ratio under different inputs

3.2 Determination of the critical sag rod position

The installation position of the sag rod and the corresponding element numbering are shown in Fig. 3(b). Based on the pretest nonlinear analysis of SCWSS for the stiffness ratio of 0.1 with the four different inputs using OpenSees [26], the variation of AAI, peak element tension ratio (maximum tension divided by the yield force), and compression ratio (maximum compression divided by the yield force) are plotted in Fig. 7 for the different sag rod positions and the four applied motions.

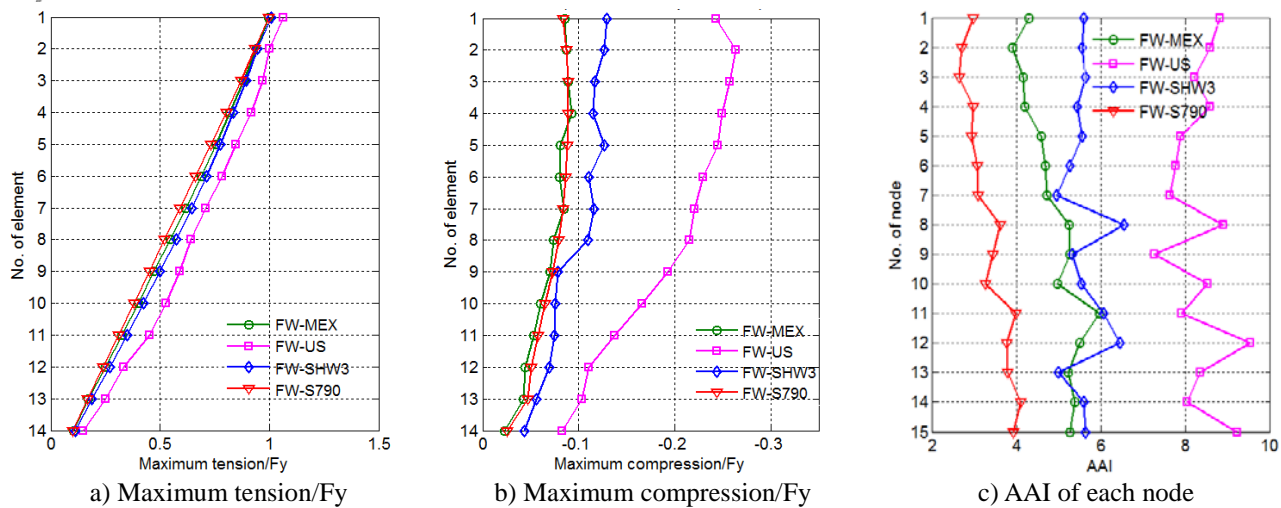


Fig. 7 – Variation of AAI and maximum tension and compression ratios under different inputs

It is observed that the maximum element tension ratio of the sag rods decreases approximately linearly from the hanging sag rod (#1) to the end sag rod (#14) under the precautionary intensity 7, and most of the sag rods remain elastic. Only sag rod 1 yields under the input of FW-US and the peak element compression ratio of the sag rods ranges from -0.08 to -0.26 ('-' means compression on sag rod) under the input of FW-US, which indicates that the sag rod elements might buckle under the FW-US input due to possible imperfections in the sag rod manufacturing process and due to the presence of eccentric loading. The buckling phenomenon has been observed and evaluated using HS tests, as discussed in the following section. The peak AAI of each node fluctuates from 8.8 at node 1 to 9.3 at node 15, with the maximum AAI of 9.6 at node 12.

In summary, the seismic response of the SCWSS is the most severe under the input motion of FW-US with seismic amplification caused by the suspension beam to sag rod stiffness ratio of 0.1. Regarding the sag rods in different vertical positions, the inelastic behavior is first observed in the hanging sag rod #1, and therefore is chosen to be the experimental substructure in the HS, while the rest of the structure is analytically modeled.

4. Hybrid simulation (HS)

After the pretest analytical study, HS tests were performed to evaluate the vertical seismic performance of the SCWSS. According to the parametric study results, conducted HS tests employed a stiffness ratio of 0.1 and sag rod #1 is simulated as the experimental substructure with the other components analytically simulated in OpenSees [26]. The HS tests were conducted with FW-US as input for three different intensity scenarios.

4.1 Test setup and specimen

Fig. 8 illustrates the main components of the utilized HS system at the Structures Laboratory of the University of California, Berkeley. It includes: (a) the computational platform OpenSees [26] which conducts the state determination for the analytical substructures and performs the numerical integration, (b) the middleware OpenFresco [28], which provides the communication between OpenSees and the PI660HybridSim, (c) PI660HybridSim, a new interface software developed within the Pacific Instruments (PI) Data Acquisition (DAQ) system that communicates with OpenFresco [28] through a TCP/IP connection, (e) DSP card which establishes the communication between the PI660HybridSim and the controller, (e) controller that controls the hydraulic actuators, and (f) MTS 311.11 loading frame with a force capacity of 44.8 kN. It is noted that the employed HS system is capable of communicating with computational platforms other than OpenSees [26], which is utilized herein for its relevance to the studied system.

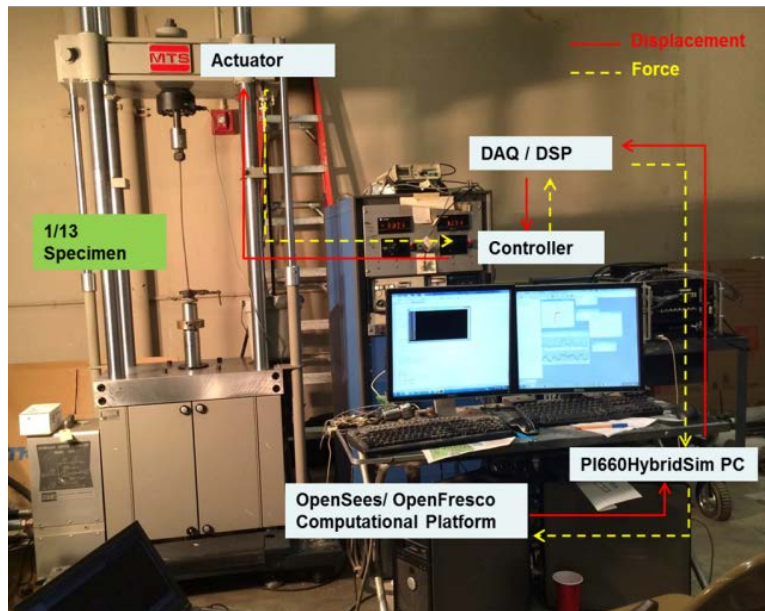


Fig. 8 – Employed HS system and setup

Considering the setup capacity and the test purpose, the test specimens shown in Fig. 9 were designed to meet the requirements of force-displacement similitude, with a scale factor of 13.0 for length and 89.3 for area. It is noted that this distorted similitude was required to maintain the relationship between the yield displacement and force of the prototype and those of the specimen and to have a specimen with the same slenderness as the prototype. Material tests of the specimen were conducted before the HS to validate the usage of the employed scale factors. Fig. 10 illustrates the force-displacement relationships of the specimen and the prototype material, and the resulting scale factors are listed in Table 2.



a) Before test b) Broken

Fig. 9 – Test specimen

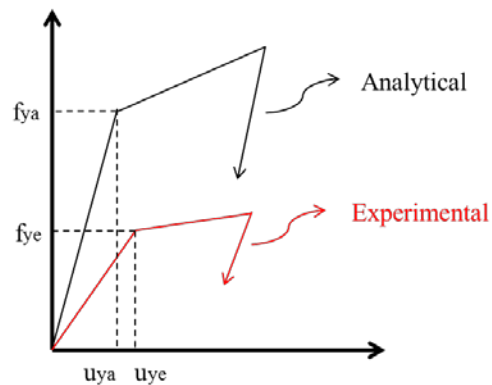


Fig. 10 – Force-deformation relationships for experimental and analytical elements

Table 2 – Scale factors used in the specimen design

Physical quantity	Elastic modulus	Stress	Density	Force	Deformation	Area	Length
Scale factor	3.1	1.5	1.0	132.5	6.25	89.3	13.0

4.3 Test results

The inputs for the HS tests are the maximum vertical floor acceleration of Zone 8 CW system, extracted from the nonlinear analysis of the main structure under the Borrego mountain earthquake, Table 1, in three different

intensity scenarios, namely frequent (FW-US_freq), precautionary (FW-US_prec) and rare (FW-US_rare) earthquakes. Fig. 11 shows the time history and the pseudo-acceleration response spectrum of these motions with the peak floor acceleration of 0.11 g, 0.30 g and 0.66 g, respectively.

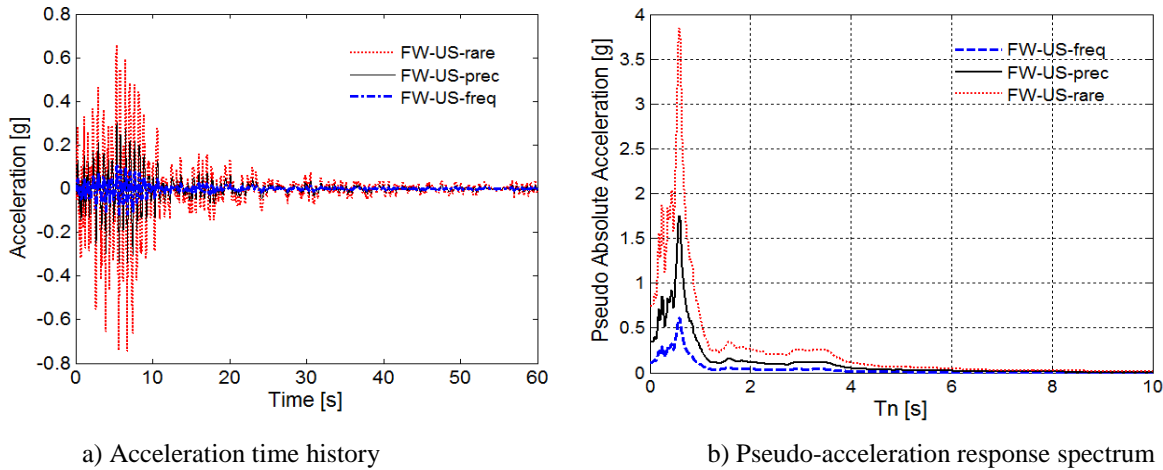


Fig. 11 – Acceleration time history and pseudo-acceleration response spectrum of the test inputs

Fig. 12 shows the time history of acceleration, velocity and displacement of nodes 2 and 15, under the inputs of FW-US_freq, from pure analytical and HS test, where the HS results match well with the analytical ones, when the specimen is elastic. The time history of acceleration, velocity and displacement of nodes 2 and 15, under the inputs of FW-US_rare, are plotted in Fig. 13, where the HS results are consistent with the analytical results when the test specimen is responding in the linear elastic range, but differences appear after yielding, which are larger in compression, due to the buckling of test specimen and other inelasticity sources that were not considered in pure analysis. These differences indicate the inadequacy of pure elastic analysis and highlight the need to conduct HS. During the test of FW-US_rare, the specimen broke after yielding, as shown in Fig. 8 leading to the abrupt termination of the time histories in Fig. 12.

Fig. 14 plots the force-displacement relationships of the experimental element from the HS test and pure analysis, under the three inputs of FW-US_freq, FW-US_prec and FW-US_rare. It is noted that the specimen buckled under the input of FW-US_rare, which is expected to subject the CW panels to much larger vertical relative displacement, 64.5 mm in full-scale as shown in Fig. 13, than the one observed in the shaking table tests (maximum of 9.8 mm in the rare condition) [21] and is expected to result in possible damage to the CW panels, which is not captured by the shaking table tests.

5. Conclusions

Due to the vulnerability of CW systems in earthquakes and the unique design of zonal hanging CW system in Shanghai Tower, the vertical seismic performance of the CW supporting system (CWSS) is a subject that requires detailed exploration. Therefore, this paper focused on the effect of the suspension beam stiffness on the vertical seismic performance of the CWSS. For this purpose, a parametric study and HS tests were performed utilizing a simplified 2D model. The following is a summary of key conclusions from the study:

- (1) The fundamental period of the simplified CW supporting structure (SCWSS) decreases from 3.66 s to 0.35 s, with the suspension beam stiffness ratio changing from 1/640 to 25.6.
- (2) Considering the maximum AAI and the peak rod deformation, the stiffness ratio of 0.1 represents the most critical CWSS configuration.
- (3) Regarding the response of the sag rod in different vertical positions, the sag rod in hanging position shows nonlinear behavior prior to other sag rods according to the parametric study.
- (4) From the comparison using the time history of acceleration, velocity and displacement between HS tests and pure analysis, HS tests show consistency with pure analysis, when the specimen remains elastic.

- (5) Due to uncaptured buckling and other inelasticity sources, inconsistent results are obtained between the HS tests and pure analysis after the specimen exhibits nonlinear behavior, particularly due to buckling.
- (6) The tested specimen buckled during the input of FW-US_rare and the consequent peak vertical deformation of the tested specimen in full scale extends to 64.5 mm, which is expected to subject the CW panel to compression and may result in possible damage.
- (7) To further investigate the seismic behavior of the whole CW system, the probabilistic performance-based analysis [29-30] should be conducted which states the performance measures in terms of the interest of relevant stakeholders.

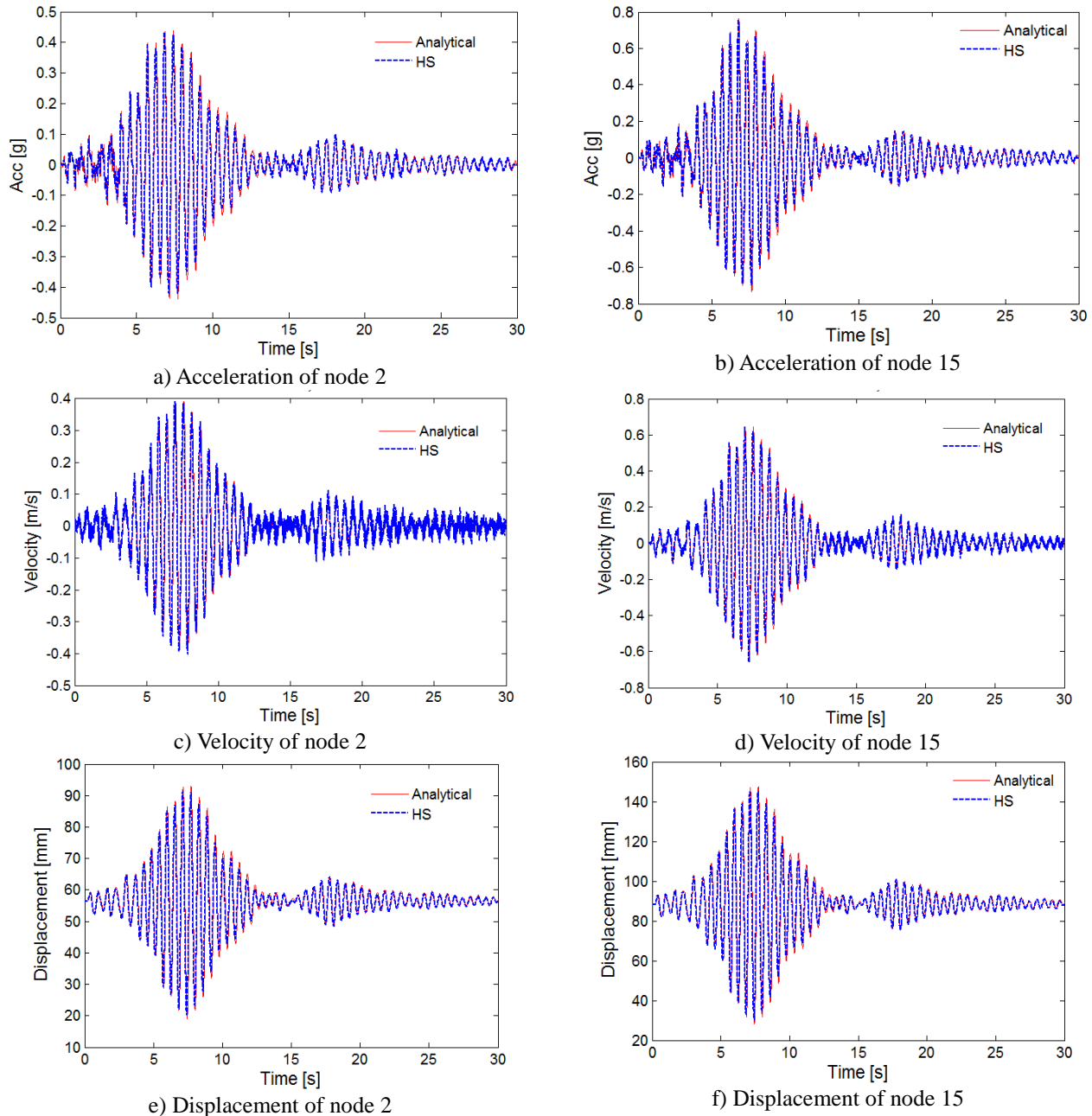


Fig. 12 – Acceleration, velocity and displacement time history of nodes 2 and 15, under the inputs of FW-US_freq, from HS and pure analytical simulation

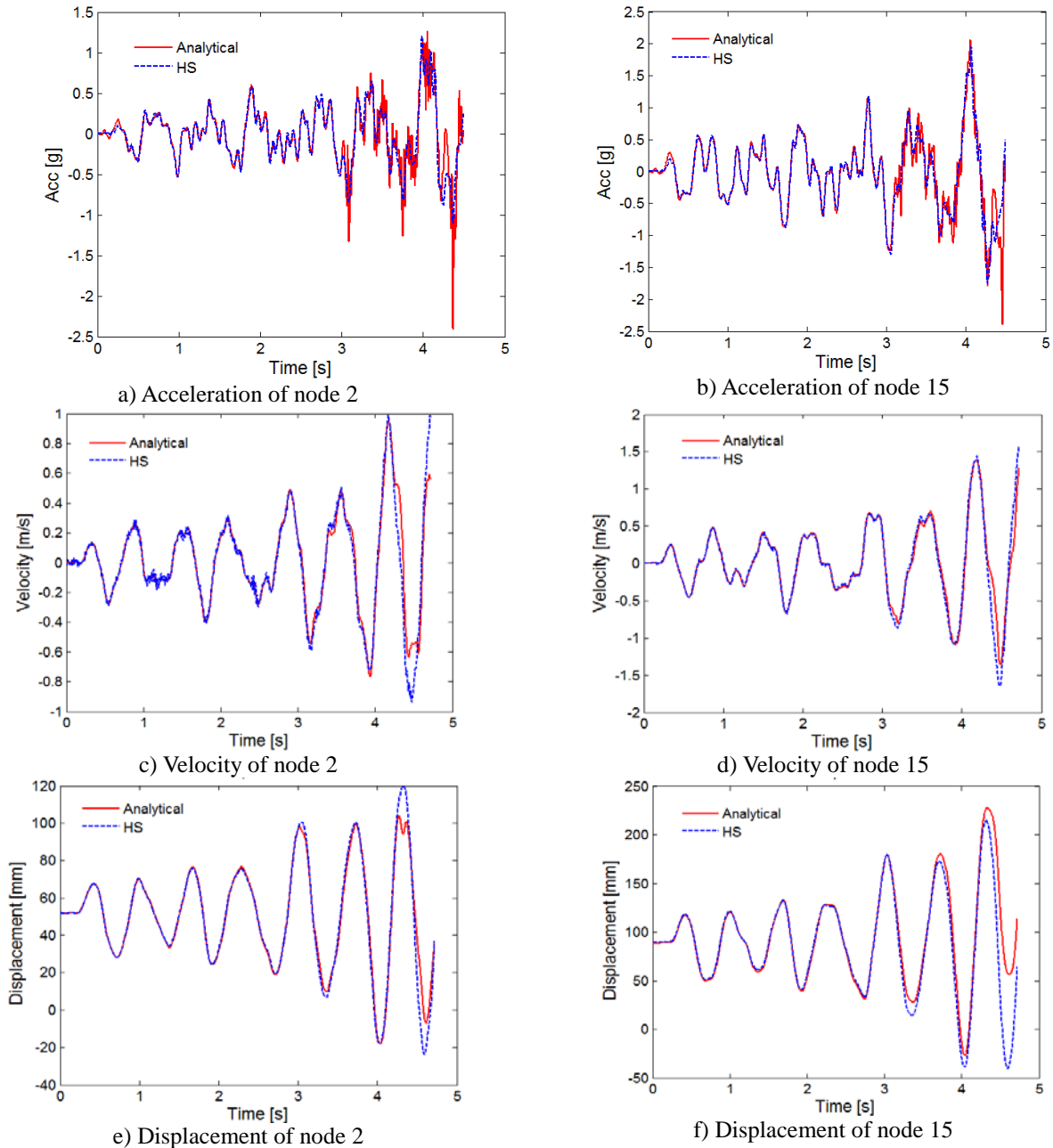


Fig. 13 – Acceleration, velocity and displacement time history of nodes 2 and 15, under the inputs of FW-US_rare, from HS and pure analytical simulation

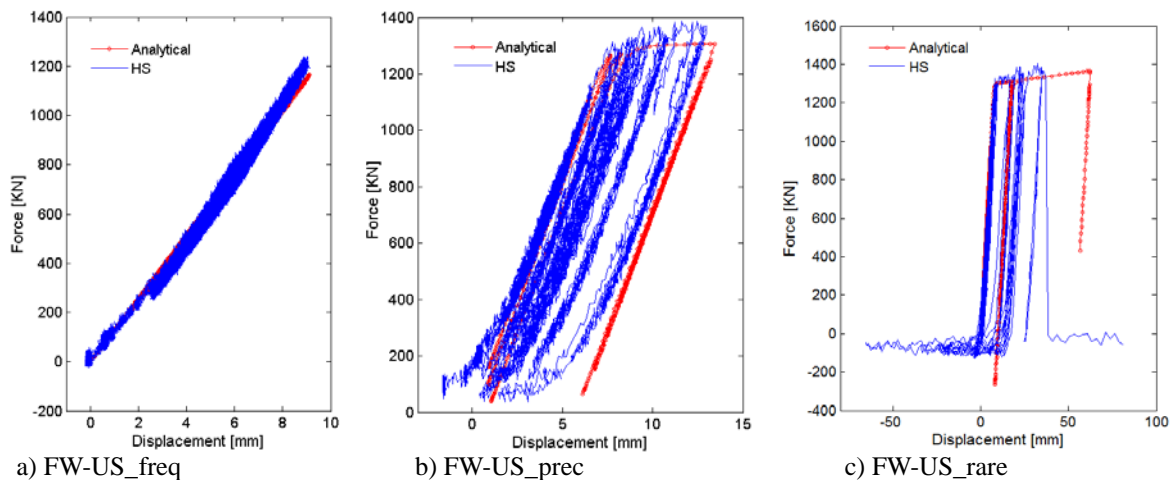


Fig. 14 – Force-displacement relationships of the experimental element from HS test and pure analysis

6. Acknowledgements

The authors are grateful for the support from the Structures Laboratory of the University of California, Berkeley, and the State Key Laboratory of Disaster Reduction in Civil Engineering in Tongji University.

7. References

- [1] Poon D, Lew P, Zhi Y, Tse B, Jain V (2010). Unique complexities of the Shanghai center curtain wall support system. In Structures Congress. PP. 2011-2020.
- [2] Miranda E (2006). Assessment of seismic acceleration demands on buildings and nonstructural components. Seminar, University of Naples "Federico II", 15th November 2006.
- [3] Memari AM (2013). Review of the performance of glazing systems in earthquakes and recent developments to mitigate damage. In Forensic Engineering 2012, Gateway to a Safer Tomorrow (pp. 123-132). ASCE.
- [4] Baird A, Palermo A, Pampanin S (2011). Facade damage assessment of multi-storey buildings in the 2011 Christchurch earthquake. *Bulletin of the New Zealand Society for earthquake engineering*, 44(4), 368-376.
- [5] Memari AM, Shirazi A, Kremer PA, Behr RA (2014). Seismic vulnerability evaluation of architectural glass in curtain walls. *Journal of Civil Engineering and Architecture Research*, 1(2), 110-128.
- [6] Broker K, Fisher S, Memari AM (2012). Seismic racking test evaluation of silicone used in a four-sided structural sealant glazed curtain wall system. In Durability of Building and Construction Sealants and Adhesives: 4th Volume. ASTM International.
- [7] Simmons NC, Memari AM (2013). Racking performance analysis of four-sided structural sealant glazing curtain wall systems. Through Video Capture Technique. AEI, 725-734, ASCE 2013.
- [8] Behr RA, Belarbi A, Culp JH (1995). Dynamic racking tests of curtain wall glass elements with in-plane and out-of-plane motions. *Earthquake engineering & structural dynamics*, 24(1), 1-14.
- [9] American Architectural Manufacturer's Association (2009a). Recommended static testing method for evaluating curtain wall and storefront systems subjected to seismic and wind induced interstory drift, Report AAMA 501.4-09, Schaumburg, IL.
- [10] American Architectural Manufacturer's Association (2009b). Recommended dynamic test method for determining the seismic drift causing glass fallout from a wall system, Report AAMA 501.6-09, Schaumburg, IL.
- [11] IBC, I. (2009). International building code. International Code Council, Inc. (formerly BOCA, ICBO and SBCCI), 4051, 60478-5795.

- [12] American Society of Civil Engineers. ASCE/SEI 7-05 (2002): Minimum design loads for buildings and other structures.
- [13] Wang Y L, LU WS, Mosalam K M (2015). Multi-modal shaking table testing for inner-skin curtain wall system of Shanghai Tower. *6th International Conference on Advances in Experimental Structural Engineering*, Illinois, U.S.
- [14] Cao LN, Lu WS, Huang BF (2010). Study on earthquake actions to glass curtain walls of a high-rise building. *Structural Engineers*, **26**(6), 142-159.
- [15] Lu W, Huang B (2008). Study on the shaking table test methods of architectural curtain walls. *Journal of Disaster Prevention and Mitigation Engineering*, **28**(4), 447-453. (in Chinese)
- [16] Takanashi K, Udagawa K, Seki M, Okada T, Tanaka H, 1975, Non-linear earthquake response analysis of structures by a computer-actuator on-line system (details of the system). *Trans. of the Architectural Institute of Japan*, **229**, 77-83.
- [17] Lee SK, Park EC, Min KW, Lee SH, Chung L, Park JH (2007). Real-time hybrid shaking table testing method for the performance evaluation of a tuned liquid damper controlling seismic response of building structures. *Journal of Sound and Vibration*, **302**(3), 596-612.
- [18] Dong B, Sause R, Ricles JM (2016). Seismic response and performance of a steel MRF building with nonlinear viscous dampers under DBE and MCE. *Journal of Structural Engineering*.
- [19] Cha Y J, Zhang J, Agrawal AK, Dong B, Friedman A, Dyke SJ, Ricles J (2013). Comparative studies of semiactive control strategies for MR dampers: pure simulation and real-time hybrid tests. *Journal of Structural Engineering*, **139**(7), 1237-1248.
- [20] Shao W, van de Lindt JW, Bahmani P, Pang W, Ziaei E, Symans MD, Dao T (2014). Real time hybrid simulation of a multi-story wood shear wall with first-story experimental substructure incorporating a rate-dependent seismic energy dissipating device. *Smart Structures and Systems*, **14**(6), 1031-1054.
- [21] Li J, Spencer Jr BF, Elnashai AS, Phillips BM (2011). Substructure hybrid simulation with multiple-support excitation. *Journal of Engineering Mechanics*, **138**(7), 867-876.
- [22] Mosalam KM, Günay S (2014). Seismic performance evaluation of high voltage disconnect switches using real-time hybrid simulation: I. System development and validation. *Earthquake Engineering & Structural Dynamics*, **43**(8), 1205-1222.
- [23] Lu WS, Huang BF, Mosalam KM, Chen SM (2016a). Experimental evaluation of a glass curtain wall of a tall building. *Earthquake Engineering & Structural Dynamics*, **45**, 1185-1205.
- [24] Lu WS, Huang BF, Chen SM, Mosalam KM (2016b). Shaking table test method of building curtain walls using floor capacity demand diagrams. *Bulletin of Earthquake Engineering*, DOI: 10.1007/s10518-016-9866-y.
- [25] He ZJ, Ding JM, Lu TT (2014). Vertical earthquake action analysis for mega frame-core tube structure of the Shanghai Tower. *Journal of Building Structures*, **01**, 27-33. (in Chinese)
- [26] McKenna F (2011). OpenSees: A framework for earthquake engineering simulation. *Computing in Science & Engineering*, **13**(4), 58-66.
- [27] National Standards of the People's Republic of China (2010). GB 50011-2010 Code for seismic design of buildings. Beijing, China Architecture & Building Press. (in Chinese)
- [28] Schellenberg A, Kim HK, Takahashi Y, Fenves GL, Mahin SA (2009). OpenFresco. University of California, Berkeley.
- [29] Günay S, Mosalam KM (2013). PEER performance-based earthquake engineering methodology, revisited. *Journal of Earthquake Engineering*, **17**(6), 829-858.
- [30] Beck JL, Porter KA, Shaikhutdinov R, Moroi T, Tsukada Y, Masuda M (2002). Impact of seismic risk on lifetime property values, Final Report, CUREE-Kajima Joint Research.